Geothermics 57 (2015) 8–17

Contents lists available at ScienceDirect

Geothermics

journal homepage: www.elsevier.com/locate/geothermics

An iTOUGH2 equation-of-state module for modeling supercritical conditions in geothermal reservoirs

Lilja Magnusdottir*, Stefan Finsterle

Lawrence Berkeley National Laboratory, Earth Sciences Division, 1 Cyclotron Road, Berkeley, CA 94720, USA

ARTICLE INFO

Article history:
Received 17 February 2015
Accepted 12 May 2015
Available online 2 June 2015

Keywords:
Supercritical water
Magmatic intrusion
High enthalpy fluids
Numerical modeling
iTOUGH2

ABSTRACT

High enthalpy geothermal fluid is becoming more desirable for energy production with advancing technology. In this study, a new equation-of-state module termed EOS1sc was developed for iTOUGH2, to provide forward and inverse modeling capabilities at supercritical conditions. As a verification exercise, test cases of five-spot geothermal problems and of a cooling pluton were studied. The IAPWS-IF97 and IAPWS-95 thermodynamic formulations were examined, and results of EOS1sc were compared to other simulators. Advantages of EOS1sc over current geothermal simulators include higher operational range for pressure and temperature, better accuracy, higher computational speed, and/or inverse modeling capabilities.

1. Introduction

Extracting supercritical fluids from geothermal reservoirs is a difficult task but it has promising possibilities for improving the economics of geothermal energy production. At temperatures and pressures above the critical point of water (374 °C and 22.064 MPa), the fluid has increased power-producing potential compared to subcritical fluids used in conventional geothermal power plants. The enthalpy is significantly higher at such high temperatures and pressures, and supercritical fluids have greatly enhanced rates of mass transfer due to the increased ratios of buoyancy forces to viscous forces in the supercritical state. Thus, more energy could be produced from a single well extracting supercritical fluids compared to a conventional geothermal well. Deeper wells would be more expensive to drill but for high enough outputs per well, drilling costs and the environmental footprint could be decreased as fewer wells need to be drilled.

There has been an increasing interest in utilizing supercritical fluids from the deep subsurface, and the feasibility of such energy extraction is likely to increase in the coming years with advancing drilling technologies. The Iceland Deep Drilling Project (IDDP) included plans of drilling geothermal wells to depths of 4–5 km in Iceland at Krafla, Nesjavellir and Reykjanes to reach supercritical fluids at temperatures of 450–600 °C, as described by Fridleifsson and Elders (2005). However, the first IDDP well drilled at Krafla in 2009 encountered 900 °C hot rhyolitic magma at a depth of only 2.1 km (Fridleifsson et al., 2010). Elders et al. (2014) discuss how this unexpected encounter with magma at a relatively shallow depth has demonstrated possibilities of higher power outputs from the contact zones of intrusions, and that it may be possible to extract energy directly from magma in the future. These observations show how a magmatic heat source could extend up to a depth shallow enough to greatly influence the hydrology and thermal behavior in the reservoir. Furthermore, these incidents are likely to become more common with increasing drilling depths in magmatic geothermal reservoirs.

In geothermal reservoir modeling, the heat source is usually assumed to be below the model's depth range, and the model is driven by boundary conditions in the bottom layer of the model. Including the heat source in the model poses a variety of modeling challenges due to the large changes in fluid properties near the critical point, and due to various unknowns such as the depth range of the water circulation and the time varying spatial distribution of the heat sources. Simulators capable of modeling supercritical conditions include HYDROTHERM (Hayba and Ingebritsen, 1994) and the HOTH2O extension to the STAR simulator (Pritchett, 1995). HYDROTHERM can simulate temperatures up to 1200 °C and pressures up to 1000 MPa, and the HOTH2O extension to STAR operates for temperatures up to 800 °C and pressures up to 100 MPa. In HYDROTHERM, a large lookup table is used to provide fluid densities, viscosities, and temperatures. The lookup table is calculated from steam-table routines of Haar et al. (1984), which were adopted by the International Association for the Properties of Water and Steam (IAPWS) in 1984. The equations by Haar et al. (1984) were later found to manifest substantial weaknesses close

* Corresponding author. Tel.: +1 510 486 6878.
E-mail address: lmagnusdottir@lbl.gov (L. Magnusdottir).

http://dx.doi.org/10.1016/j.geothermics.2015.05.003
0375-6505/

to the critical point and when the equations were extrapolated beyond their operational range (Wagner and Pruss, 2002). Cooling plutons and hydrothermal systems on mid oceanic ridges have been modeled using HYDROTHERM (Hayba and Ingebritsen, 1997; Ingebritsen et al., 2010). However, both HYDROTHERM and STAR are limited to rectangular or radial grids, thus imposing restrictions in representing the complex geometry of magmatic geothermal reservoirs.

Other simulators that have been extended to supercritical conditions and are capable of modeling irregular computational grids include the Complex System Modeling Platform CSMP++ (Weis et al., 2014) and codes developed based on the TOUGH2 suite of nonisothermal multiphase flow simulators (Pruess, 1991). The TOUGH2-based codes include the supercritical equation-of-state module by Brikowski (2001), the supercritical equation-of-state module by Kissling (2004), and the AUTOUGH2 code developed at the University of Auckland (Croucher and O'Sullivan, 2008). In AUTOUGH2, the IAPWS-IF97 thermodynamic formulation (Wagner et al., 2000) is used, and the IFC-67 formulation (International Formulation Committee of the 6th International Conference on the Properties of Steam, 1967) is used both in standard TOUGH2, iTOUGH2 and the supercritical version of TOUGH2 by Kissling (2004).

The operational ranges tested and accepted by IAPWS for water's thermodynamic formulations are summarized in Table 1. The IFC-67 formulation is accepted by IAPWS for up to 800 °C and 100 MPa, whereas the IAPWS-IF97 and IAPWS-95 (International Association for the Properties of Water and Steam, 2009) formulations are significantly more accurate for supercritical conditions (Wagner et al., 2000). Due to the inaccuracy of IFC-67 close to the critical point, the operational limit of temperature is set as 350 °C in TOUGH2 and iTOUGH2. IAPWS-95 operates up to 1000 °C and 1000 MPa, and the revised version of the IAPWS-IF97 formulation operates up to 800 °C for pressures up to 100 MPa, and to 2000 °C for pressures up to 50 MPa (International Association for the Properties of Water and Steam, 2007). The temperature of basaltic magma can reach more than 1200 °C, so in order to be able to answer questions relevant to the field management of magmatic geothermal systems, it is important to develop a simulator that can accurately model the high pressures and temperatures of these magmatic intrusions.

This paper describes how the applicability of the iTOUGH2 simulator was extended to supercritical conditions. In the iTOUGH2 simulator, irregular computational grids can be modeled. Moreover, iTOUGH2 provides capabilities for sensitivity, uncertainty, and inverse modeling analyses, which can be used to examine the relevance of supercritical properties and processes, and to calibrate magmatic geothermal reservoir models. Hence, this extended version of iTOUGH2 can be used to model magmatic intrusions, and some of the unknown model parameters can be estimated using inverse analysis.

First, the IAPWS-IF97 and IAPWS-95 formulations are described. The IAPWS-95 formulation can be extrapolated to extremely high temperatures and densities above the operational limit accepted by IAPWS, as described by Wagner and Pruss (2002). Yamazaki and Muto (2004) describe how extrapolating the original IAPWS-IF97 formulation to higher temperatures and pressures is limited; we examine here the possibility of extrapolating the extended revised version of IAPWS-IF97. The IAPWS-IF97 and IAPWS-95 formulations are compared by studying a geothermal five-spot problem described by Pruess (1991) for conditions below the critical point, close to the critical point, and for very high temperatures above the critical point. Then, the new EOS1sc module is compared to HYDROTHERM by modeling a cooling pluton with an initial temperature of 1100 °C and by studying the corresponding groundwater flow and heat transfer in the geothermal system. Finally, the inverse capabilities at supercritical conditions are demonstrated by estimating the initial temperature of the pluton and the permeability of the geothermal reservoir using observations of injection pressure, production temperature and production rate.

2. Method

The IAPWS-95 formulation serves as the international standard for water's thermodynamic properties. The IAPWS-IF97 formulation is a separate, faster formulation based on IAPWS-95. It is maintained for industrial use and replaces the IFC-67 formulation currently used in standard TOUGH2. The accuracy and speed of calculating the thermodynamic properties are improved significantly when using the IAPWS-IF97 formulation compared to using IFC-67 (Wagner et al., 2000).

The IAPWS-IF97 formulation is given in terms of five regions nominally defined as liquid, vapor, supercritical, two-phase, and high temperature vapor as shown in Fig. 1. Regions 1, 2 and 5 in Fig. 1 are individually covered by a fundamental equation for the specific Gibbs free energy given in terms of pressure and temperature. Region 3 is covered by a fundamental equation for the specific Helmholtz free energy and is given in terms of density and temperature. Region 4, i.e., the saturation curve, is given by a saturation-pressure equation. These equations are further described by the International Association for the Properties of Water and Steam (2007). In the new EOS1sc module, the supercritical equation-of-state (EOS) used in AUTOUGH2 was incorporated into iTOUGH2. In AUTOUGH2, regions 1–4 of the IAPWS-IF97 formulation were implemented into the EOS, as described by Croucher and O'Sullivan (2008). In EOS1sc, region 5 was included as well to extend the applicability of the EOS to 2000 °C for pressure at or below 50 MPa.

The IAPWS-95 formulation was also implemented into iTOUGH2 as described by Magnusdottir and Finsterle (2015). In the IAPWS-95 formulation, the primary variables are density and temperature for the entire state space. Thus, iterative function inversions are required when using IAPWS-95 outside of the supercritical region in Fig. 1. In EOS1sc, there are three options to select the thermodynamic formulation: (1) IFC-67, which is only valid for subcritical conditions, (2) IAPWS-IF97, or (3) IAPWS-IF97 for temperature below 800 °C and IAPWS-95 for temperature equal or greater than 800 °C. For the last option, IAPWS-95 is not used for the whole temperature range because IAPWS-IF97 is significantly faster and accurately approximates IAPWS-95 within its operational range of 800 °C (Magnusdottir and Finsterle, 2015).

3. Five-spot problem

A geothermal five-spot problem described by Pruess et al. (1999) was modeled using EOS1sc in iTOUGH2 to compare the thermodynamic formulations IAPWS-IF97 and IAPWS-95. The five-spot well pattern shown in Fig. 2 has a high degree of symmetry so only one-eighth of the pattern, which includes one injector and one producer, were modeled. The reservoir was modeled as a homogeneous porous medium with a thickness of 305 m, a porosity of 0.01, and a matrix permeability of 6×10^{-15} m^2. The grain density of the rock was set as 2650 kg/m^3, the specific heat was set as 1000 J/kg °C, and the heat conductivity was defined as 2.1 W/m °C (Pruess et al., 1999). No-flow Neumann boundary conditions were used.

First, a subcritical version of the problem was modeled and the IAPWS-IF97 formulation compared to the IAPWS-95 formulation as well as the IFC-67 formulation in standard TOUGH2. Then, supercritical versions were modeled with temperature and pressure close to the critical point. Finally, very high temperature and pressure are simulated, representing conditions that are likely to occur in magmatic intrusions. Yamazaki and Muto (2004) describe

Table 1
Temperature and pressure range for international thermodynamic formulations.

International standard	Simulator	Temperature range (°C)	Pressure range (MPa)
IFC-67	TOUGH2, iTOUGH2	0–800	0–100
IAPWS-95	iTOUGH2-EOS1sc	0–1000	0–1000
IAPWS-IF97	AUTOUGH2, iTOUGH2-EOS1sc	0–800	0–100
Revised region 5 of IAPWS-IF97	iTOUGH2-EOS1sc	800–2000	0–50

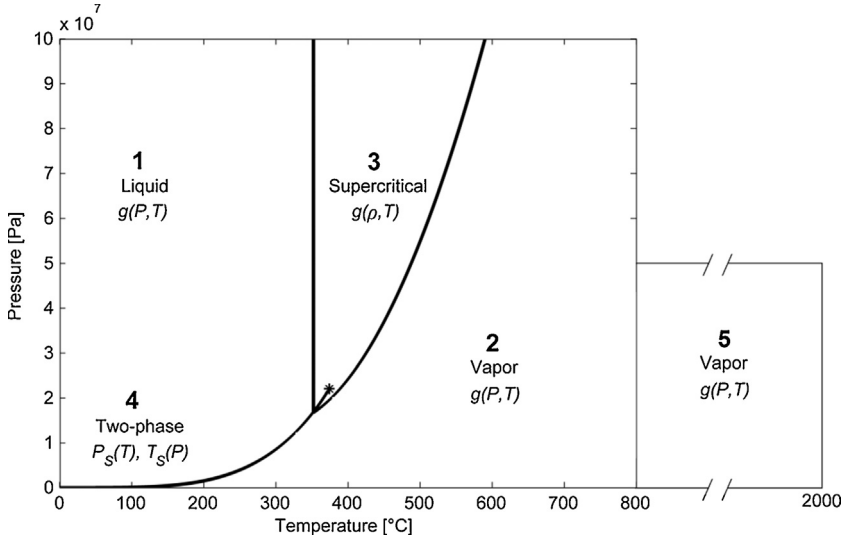

Fig. 1. Regions for the IAPWS-IF97 thermodynamic formulation.

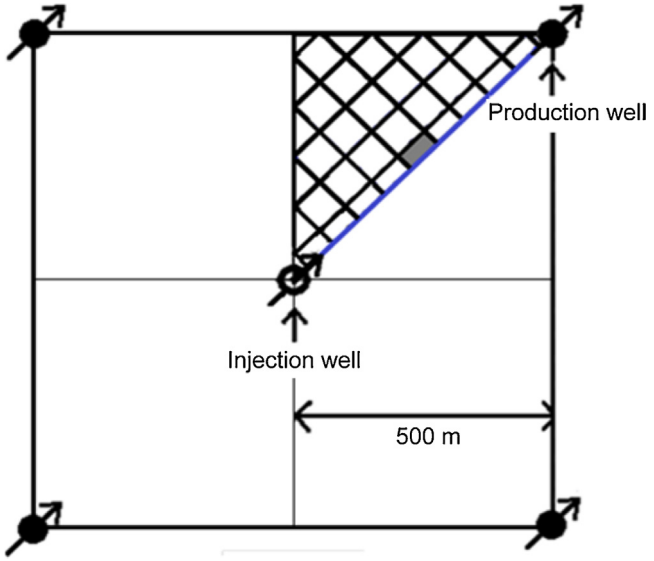

Fig. 2. Five-spot injection/production problem showing the element in the middle between the injector and producer in gray.

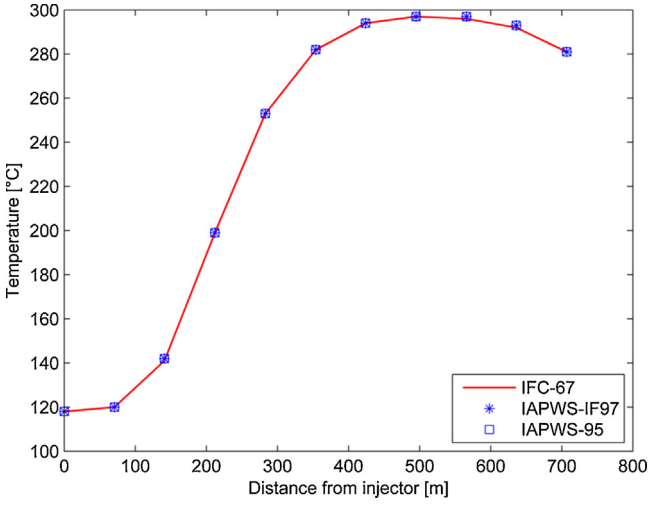

Fig. 3. Temperature profile after 36.5 years for the subcritical scenario along a line (shown in blue in Fig. 2) connecting the injector and the producer. (For interpretation of the references to colour in this figure legend, the reader is referred to the web version of this article.)

how region 2 (Fig. 1) with an operational limit of 800 °C and 100 MPa can be extrapolated to higher temperature and pressure with better accuracy than region 5 of the original IAPWS-IF97 formulation, which has an operational limit of 2000 °C for pressure below 10 MPa. However, the possibility of extending the formulation was very limited. Thus, the results when using the IAPWS-95 formulation in iTOUGH2 to model the supercritical problem were compared to those obtained when extrapolating region 2 of the IAPWS-IF97 formulation. Furthermore, the possibility of extrapolating region 5 of the revised version of IAPWS-IF97 formulation was studied and results compared to IAPWS-95.

3.1. Subcritical conditions

For the subcritical problem, the initial temperature for the reservoir was set as 300 °C, the initial pressure was set as 8.593 MPa, and the initial liquid saturation was defined as 0.99. Fluid with an enthalpy of 500 kJ/kg (118 °C) was injected into the reservoir at a rate of 24 kg/s and produced at the same rate. The reservoir was simulated using standard TOUGH2 with the IFC-67 formulation, and iTOUGH2 with the IAPWS-95 and IAPWS-IF97 formulations. Fig. 3 shows the temperature profile after 36.5 years at the elements along the line connecting the injection and production wells. All three thermodynamic formulations

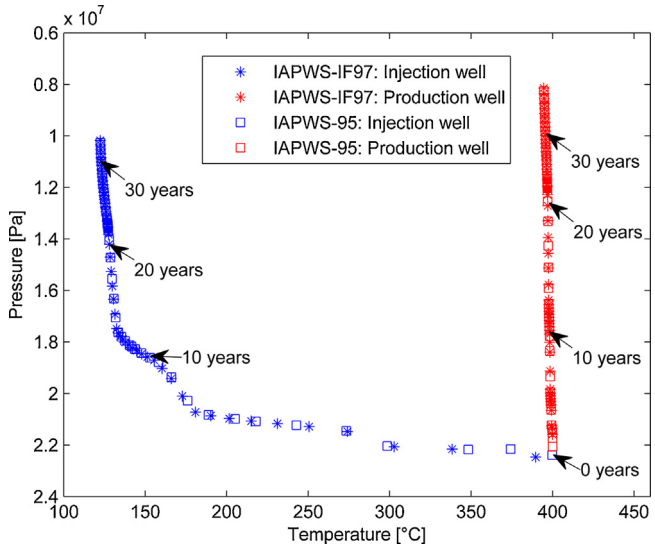

Fig. 4. Pressure-temperature diagram for the injector and the producer for supercritical conditions close to the critical point.

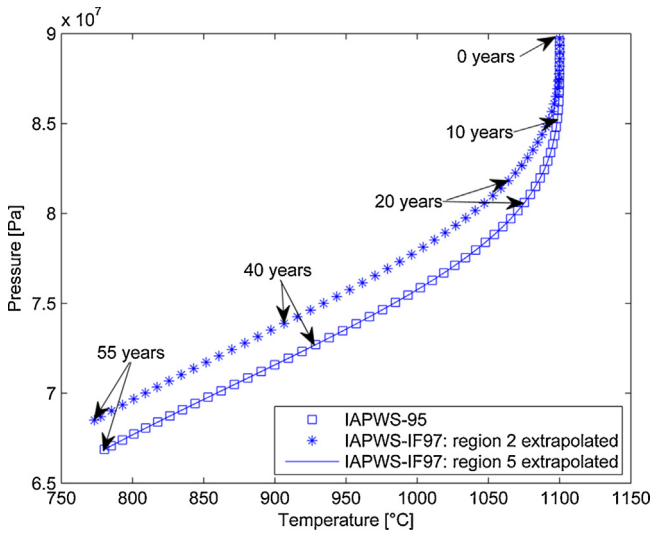

Fig. 5. Pressure-temperature diagram for the element in the middle between the injector and the producer (shown in gray in Fig. 2) for supercritical conditions with initial temperature at 1100 °C.

operate at these subcritical conditions and all simulators give equal results.

3.2. Supercritical conditions close to the critical point

The five-spot geothermal problem was modeled for supercritical conditions close to the critical point of water, which is at 374 °C and 22.064 MPa. The initial temperature of the reservoir was raised to 400 °C, and the initial pressure was increased to 22.06 MPa. The injection enthalpy of 500 kJ/kg was retained. The injection and production rates were decreased to 7.2 kg/s, which is in accordance to conditions modeled by Croucher and O'Sullivan (2008). The mass rate reported by Croucher and O'Sullivan (2008) was 0.9 kg/s, which is for the 1/8th symmetry domain instead of the total mass rate of 7.2 kg/s.

Fig. 4 shows the pressure-temperature diagram for the injector and producer modeled up to 36.5 years. In standard iTOUGH2, the IFC-67 thermodynamic formulation does only run for temperatures up to 350 °C so this case focused on comparing the IAPWS-IF97 formulation to the IAPWS-95 formulation. The results were equivalent because the IAPWS-IF97 formulation is a close approximation of the IAPWS-95 formulation. The difference in calculated thermodynamic properties is negligible between IAPWS-IF97 and IAPWS-95 at these temperatures.

3.3. Supercritical conditions with extreme pressure and temperature

In magmatic geothermal reservoirs, the pressure and temperature at great depths near magmatic intrusions can be very high. Hence, the previously studied five-spot problem was also modeled for extreme pressure and temperature conditions. The applicability of the IAPWS-IF97 thermodynamic formulation compared to the IAPWS-95 formulation was studied. The injection and production rates were set as 48 kg/s, and the enthalpy of the injected fluid was set as 3000 kJ/kg. The initial temperature of the reservoir was set as 1100 °C, and the initial pressure was set as 90 MPa.

Yamazaki and Muto (2004) showed the limitations of extending the original IAPWS-IF97 formulation above the operational temperature range of 800 °C. Although the formulation could be extended to higher temperatures at low pressures by extrapolating region 2 (Fig. 1) instead of using region 5 of the original IAPWS-IF97 formulation, the deviation of IAPWS-IF97 from IAPWS-95 became unacceptably high for the pressures and temperatures likely to occur in magmatic intrusions. Fig. 5 shows the pressure-temperature diagram for the element located in the middle between the injector and producer for 55 years of production. Extrapolating region 2 of the IAPWS-IF97 formulation gives different results than the IAPWS-95 formulation, and the deviations in thermodynamic properties would be larger for higher temperatures (Yamazaki and Muto, 2004). Thus, region 2 of the IAPWS-IF97 formulation could not be used to accurately model such high temperatures and pressures likely to be present deep in magmatic geothermal reservoirs.

Next, the same five-spot problem was simulated by extending region 5 of the revised IAPWS-IF97 formulation and the results are equivalent to those when using the IAPWS-95 formulation (Fig. 5). The main disadvantage of using the IAPWS-95 formulation is the relatively slow computational speed. The IAPWS-IF97 formulation is significantly faster: the CPU time decreases by a factor of 10 for this case when using IAPWS-IF97 instead of IAPWS-95. However, the advantage of the IAPWS-95 formulation is that it can be extrapolated to extremely high temperatures and densities (Wagner and Pruss, 2002). Hence, the possibility of extrapolating region 5 of the revised IAPWS-IF97 formulation to even higher temperature and pressure was studied.

The initial temperature and pressure of the previous five-spot problem was increased to 1500 °C and 150 MPa. The pressure-temperature diagram for the element located in the middle between the injector and producer after 55 years of production is shown in Fig. 6. Even at such high temperature and pressure conditions, the IAPWS-95 formulation and the revised IAPWS-IF97 formulation with region 5 extrapolated give similar results. The difference in density at 1500 °C and 150 MPa between the two formulations is approximately 0.1%, and the difference in internal energy is close to 0.02%. Extrapolating region 2 to such high temperature and pressure gave unphysical thermodynamic properties, and the simulation did not converge. Thus, it is recommended to use the revised IAPWS-IF97 formulation instead of IAPWS-95 for faster computational speed and to extrapolate region 5 of the formulation if needed. However, for very high temperature and pressure conditions, it is important to study further the uncertainty of extrapolating the thermodynamic formulation.

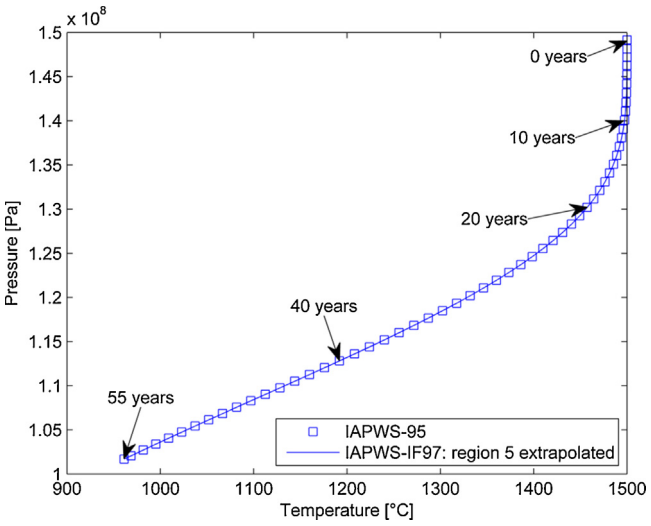

Fig. 6. Pressure-temperature diagram for the element in the middle between the injector and the producer (shown in gray in Fig. 2) for supercritical conditions with initial temperature at 1500 °C.

Table 2
Rock properties for the hydrothermal system shown in Fig.7.

Rock formation	Color	Porosity (%)	Permeability (m^2)
Impermeable layers	Gray	5	10^{-20}
Geothermal reservoir	Light green	10	10^{-14}
Surrounding formation	Dark green	10	10^{-17}
Pluton	Red	5	10^{-20}

4. Cooling pluton

4.1. Model setup

The forward and inverse capabilities of EOS1sc in iTOUGH2 were demonstrated for a cooling pluton with an initial temperature of 1100 °C. The IAPWS-IF97 formulation with region 5 extrapolated in EOS1sc was used to investigate the groundwater flow and heat transfer in the hydrothermal system as the pluton cools down, and to compare the results using iTOUGH2 to results using HYDROTHERM. Then, inverse analysis was used to estimate the initial temperature of the pluton, and the permeability of the geothermal reservoir using observations of injection pressure, production temperature, and production rate after the reservoir had reached steady-state. The model is two-dimensional with dimensions $4 \times 10\,km^2$, and a nominal thickness of 1 m. The pluton is emplaced at a depth of 2.5 km, and the dimension of the pluton is $0.5 \times 1.5\,km^2$. The rock is basalt and it consists of four regions in terms of porosity and permeability, as shown in Fig. 7. The porosity and permeability of each region are listed in Table 2.

In geothermal systems, the depth of the water circulation is usually not well known, and it differs from one field to another. Geothermal wells drilled in Iceland indicate that the water circulation is at a depth of 2–3 km with most feed zones above 2000 m below sea level. For this model, the geothermal system is restricted by impermeable layers ($k = 10^{-20}\,m^2$) on the vertical boundaries and at a depth of 3.5 km (shown in gray in Fig. 7). Additionally, a 300 m thick cap rock is modeled at a depth of 200 m, and the permeability of the cap rock (gray) as well as the pluton (red) is $k = 10^{-20}\,m^2$. The permeable formation in the reservoir is divided into two regions: the geothermal system (light green) and the less permeable surrounding formation (dark green). The grain density of the basalt rock is set as $2600\,kg/m^3$, the thermal conductivity is set as 2 W/(m K), and the heat capacity is set as 1000 J/(kg K) (Clauser and Huenges, 1995; Bouhifd et al., 2007).

The surface temperature and pressure were set constant at 20 °C and 1 atm (0.101325 MPa). Dirichlet boundary conditions were implemented by assigning very large volumes ($V = 10^{50}\,m^3$) to the grid blocks on the boundaries. That way, the thermodynamic conditions do not change from fluid or heat exchange with the adjacent blocks. A temperature gradient of 100 °C/km and hydrostatic pressure were modeled. The initial temperature of the pluton was set as 1100 °C, and the initial pressure was defined approximately 10% less than lithostatic pressure. Therefore, the initial pressure of the pluton is significantly higher than the hydrostatic pressure of the surrounding geothermal system. The pluton temperature on the bottom boundary is fixed at 1100 °C, thus assuming that there is a heat source beneath from which the pluton intruded. For a geothermal reservoir, the true hydrothermal behavior on the model boundaries might not be known but the new EOS1sc module in iTOUGH2 could be used to determine the appropriate boundaries. The EOS1sc module can more accurately represent the flow of supercritical fluid than the EOS1 module. However, it is also important to note that numerous simplifying assumptions are used in this model. These include the assumptions that the fluid is pure water and that there is no contribution from magmatic fluids. The effect of the brittle-ductile transition in the rock and the pluton's latent heat of crystallization are also not accounted for. These assumptions will be tested in the future by adding relevant features to iTOUGH2.

4.2. Steady-state simulation

First, the forward problem is studied of the pluton cooling down until the reservoir reaches steady state. The temperature distribution 5000 years after the magma intrusion is shown in Fig. 8. The geothermal system is highly permeable ($k = 10^{-14}\,m^2$) which results in heat transfer dominated by advection. The density-driven fluid migration is rapid, and an upwelling plume with temperatures higher than 250 °C forms directly above the cooling pluton. For comparison, the same case was modeled using HYDROTHERM; the absolute difference in temperature results at 5000 years is shown in Fig. 9. Both simulators show similar temperature distributions with an absolute difference in temperature less than 1 °C. In HYDROTHERM, pressure and enthalpy uniquely specify the thermodynamic state in the single-, two-phase, and supercritical regions instead of switching the dependent variables based on the phase of the fluid. Thus, instead of the IAPWS-IF97 formulation implemented in iTOUGH2, a large lookup table calculated from steam-table routines of Haar et al. (1984) is used in HYDROTHERM to provide fluid densities, viscosities, and temperatures. The equations by Haar et al. (1984) have been found to manifest weaknesses close to the critical point (Wagner and Pruss, 2002). Additional differences between HYDROTHERM and iTOUGH2 include the elements being limited to regular rectangular or radial computational grids in HYDROTHERM because the finite difference method is used. In iTOUGH2, the integral finite difference method is used which allows for irregular, unstructured computational grids. However, differences due to different computational grids were avoided in this comparison by using a rectangular grid of 80×40 elements for both simulators.

The temperature distribution at 100.000 years as well as fluid flow vectors and the location of elements 212, 2440, and 2452 are shown in Fig. 10. The maximum pore velocity at 5000 years is 18 m/yr. At 100.000 years it has decreased to 15 m/yr. Once the intrusion has cooled down, heat is conducted from the heat source below the intrusion where the temperature of the elements is fixed at 1100 °C. The fluid vectors in Fig. 10 show how the heated water rises and heats up the rock above the pluton where it cools down, creating the buoyancy-driven circulation. In addition,

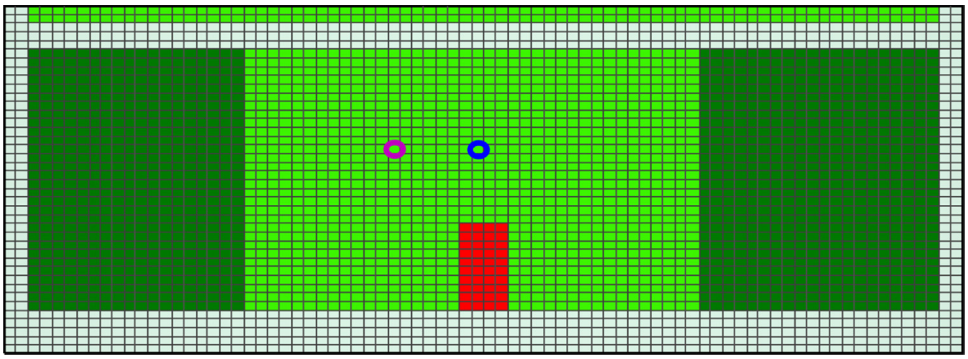

Fig. 7. Rock formations. The geothermal reservoir is shown in light green, the surrounding formation in dark green, the pluton is shown in red, and the impermeable layers are shown in gray. The circles represent the location of the injector (magenta) and the producer (blue).

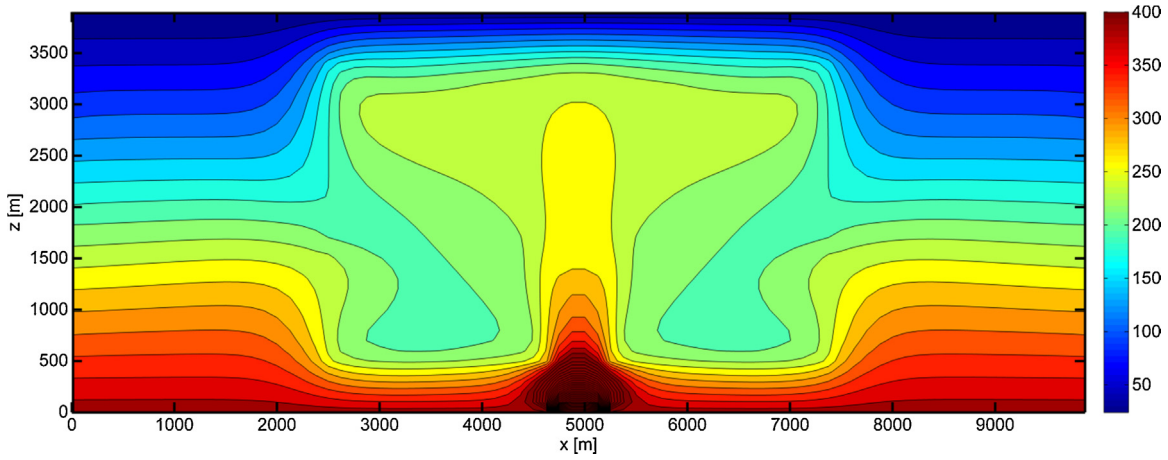

Fig. 8. Temperature distribution (°C) at 5000 years after the intrusion. The maximum temperature at elements below the intrusion reaches 1100 °C, but the color bar has been set to a maximum temperature of 400 °C.

smaller circulations of water form deep at the vertical edges of the geothermal system. The permeability of the formation surrounding the geothermal system is lower than that of the geothermal reservoir, causing a slower decline in temperature in the formation.

Fig. 11 shows the temperature histories for the elements circled in Fig. 10 for up to 100,000 years after the intrusion. The temperatures of the elements that are located closer to the surface (elements 2440 and 2452), increase rapidly due to the upwelling plume of hot water. The element located closer to the bottom boundary of the system (element 212) cools down as heat is conducted to the geothermal system. After approximately 10,000 years, the temperatures of the elements have reached a meta-stable state. The temperature histories from iTOUGH2 are equivalent to the ones from HYDROTHERM until after about 30,000 years. Then, the highs and lows of the temperature perturbation occur a little earlier in HYDROTHERM than in iTOUGH2, and the difference increases with time. In order to minimize computational errors, the computational grid might have to be refined. However, apart from the timing of

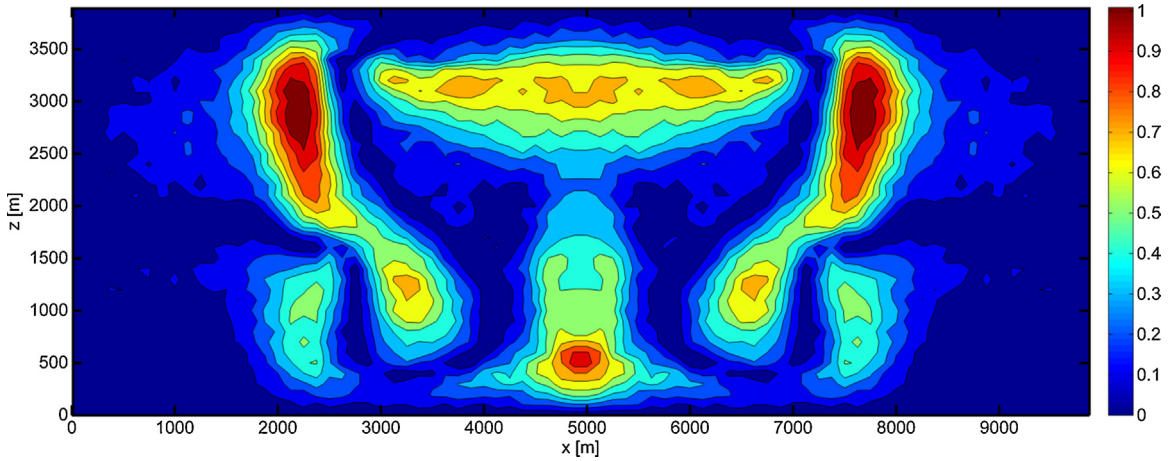

Fig. 9. Absolute difference between the temperature results (°C) from iTOUGH2 and HYDROTHERM at 5000 years after the intrusion.

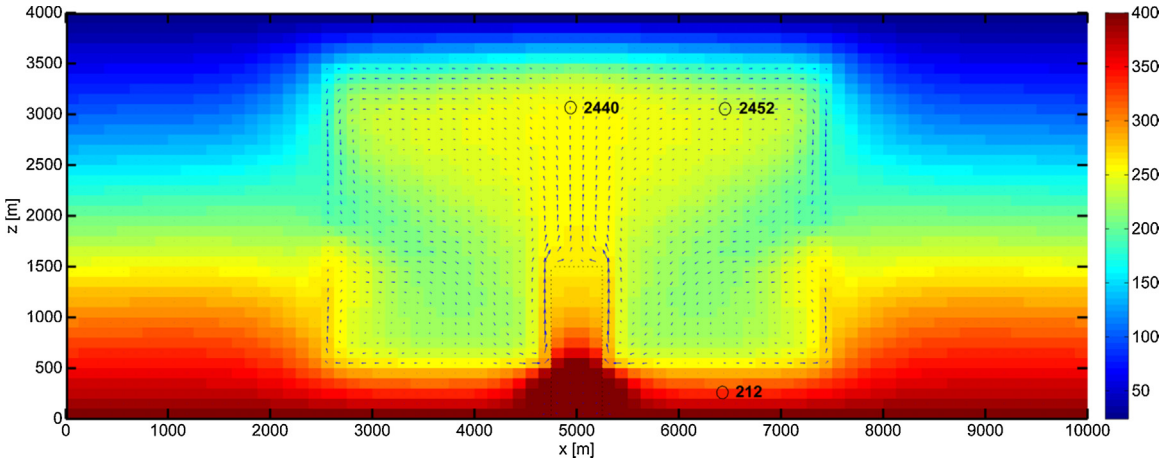

Fig. 10. Temperature distribution (°C) and flow vectors at 100,000 years after the intrusion. Elements 212, 2440, and 2452 are circled. The maximum temperature at elements below the intrusion reaches 1100 °C but the colorbar has been set to a maximum temperature of 400 °C.

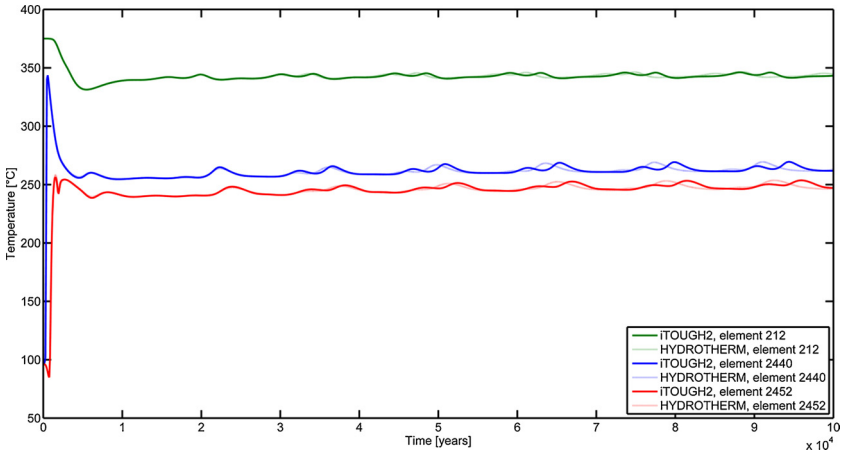

Fig. 11. Temperature histories for elements 212, 2440, and 2452 (element locations are shown in Fig. 10).

these perturbations after 30,000 years, both simulators are showing a similar temperature behavior.

4.3. Inverse analysis

iTOUGH2 provides a variety of analysis options for the TOUGH2 simulator, including (1) parameter estimation by automatic history matching (also referred to as inverse modeling), (2) local and global sensitivity analyses for quantifying the influence of input parameters on output variables, and for the selection of influential parameters and sensitive observations, (3) uncertainty propagation analysis for the estimation of prediction uncertainties as a result of input uncertainties, and (4) data-worth analysis for the identification of the most valuable (actual and potential) data set with respect to its ability to reduce estimation or prediction uncertainty. Any input parameter to the TOUGH2 model can be considered unknown or uncertain, including hydrological and thermal properties, initial and boundary conditions, as well as geometric and geostatistical parameters (Finsterle and Kowalsky, 2008). The influence of these parameters or their value can be estimated using any type of data for which a corresponding TOUGH2 output is calculated.

The analysis options of iTOUGH2 are available for any TOUGH2 module, or any external software that can be run without user intervention using text-based input and output files (Finsterle and Zhang, 2011a). The purpose of this section is to briefly demonstrate the integration of the newly developed EOS1sc module into the iTOUGH2 simulation-optimization framework – a comprehensive analysis of a high-temperature geothermal system using iTOUGH2 will be described in a future communication.

Here, we simply perform an inversion of synthetically generated exploitation data from the system previously described in Section 4.1. Fluid with an enthalpy of 500 kJ/kg is injected at a constant rate of 1 kg/s (this rate is small as only a one-meter wide, two-dimensional model domain is considered); the injection pressure is monitored. Temperature and extraction rates are observed in a production well located above the intrusion (see Fig. 7 for well locations). The pressure, temperature, and production-rate data are corrupted by Gaussian noise with standard deviations of 2 bars, 3 °C, and 0.1 kg/s, respectively. Data are collected monthly during the first 5 years of production. The calibrated model is then used to predict reservoir performance for an additional 15 years.

For this demonstration, the logarithm of reservoir permeability and initial pluton temperature are considered the unknown parameters to be estimated by history matching. Since the initial pluton temperature is updated during the inversion, a natural-state calculation starting from the time of the intrusion is needed, followed by a simulation of the transient behavior during reservoir exploitation.

The parameters are estimated by solving a non-linear weighted least-squares problem by performing five iterations of the

Table 3
Results of parameter estimation.

	$\log_{10}(k(\mathrm{m}^2))$	T_{pluton} (°C)
True value	−14.000	1100.0
Initial guess	−14.500	1400.0
Best estimate	−14.004	1097.3
Estimation uncertainty	0.009	6.6
Composite sensitivity	2104.2	182.3
Correlation coefficient	−0.28	
Parameter independence measure	0.96	0.96

Levenberg–Marquardt minimization algorithm. Estimation and prediction uncertainties are approximately calculated assuming the model is linear within the confidence region, and the errors are normally distributed.

Table 3 summarizes information about the unknown parameters, including composite sensitivity measures, estimation uncertainties, parameter independence measure, and correlation coefficients. All these measures are calculated by iTOUGH2; for definitions and interpretations, see Finsterle and Zhang (2011b). The estimated parameters are consistent (accounting for their estimation uncertainty) with the parameter values used to generate the synthetic data. The composite influence measure, which is the sum of the absolute values of the scaled sensitivity coefficients, suggests that permeability is more influential on the observed system behavior than the initial pluton temperature. This high impact of permeability stems mainly from the sensitivity of injection pressures; the production temperature (arguably the more relevant prediction variable) is similarly affected by permeability and the initial pluton temperature. Note that the sensitivity analysis is local in the sense that it applies to the conditions at the optimum parameter set. Finsterle et al. (2013) describe an application (in the context of geothermal reservoir engineering) of iTOUGH2's global sensitivity analysis methods, which examine sensitivities over the entire feasible parameter space. The two parameters are negatively correlated, indicating that a similar system response (as represented by the calibration data) can be obtained by increasing permeability and concurrently reducing pluton temperature. iTOUGH2 also calculates an overall measure of parameter independence, which is the ratio of the estimation uncertainty of a parameter if it were determined by itself and that when determined jointly with other parameters. The value of 0.96, which is close to 1.0, indicates that estimation uncertainty is only slightly increased due to parameter correlations.

Table 4 summarizes a subset of the information about the observations and residuals calculated by iTOUGH2. The composite sensitivity measures of the calibration data show the large information content of the injection pressure for the estimation of the uncertain input parameters, specifically reservoir permeability. The production rate is not very sensitive, as it is largely constrained by the specified injection rate. The residual analysis shows that the final match to the data is consistent with the expectation, i.e., the mean residuals are close to zero, their standard deviations are similar to the measurement noise, and the slope of a linear regression of the observed versus calculated data is close to one. There is a bias in the temperature residuals, which also leads to a low coefficient of determination; this bias persists throughout the 15-year prediction phase. Additional iterations appear to be needed to remove this bias. Each data set contributes approximately one-third to the objective function, indicating a good balance. Measuring injection pressure and production temperature is equally worthwhile for solving the inverse problem at hand, while production rate contributes less to the determination of permeability and pluton temperature. Assuming we are mainly interested in predicting the temperature decline during long-term exploitation, measuring the production temperature receives by far the highest data worth (as expected). For a detailed explanation of results from a data-worth analysis, see Dausman et al. (2010) and Wainwright and Finsterle (2015).

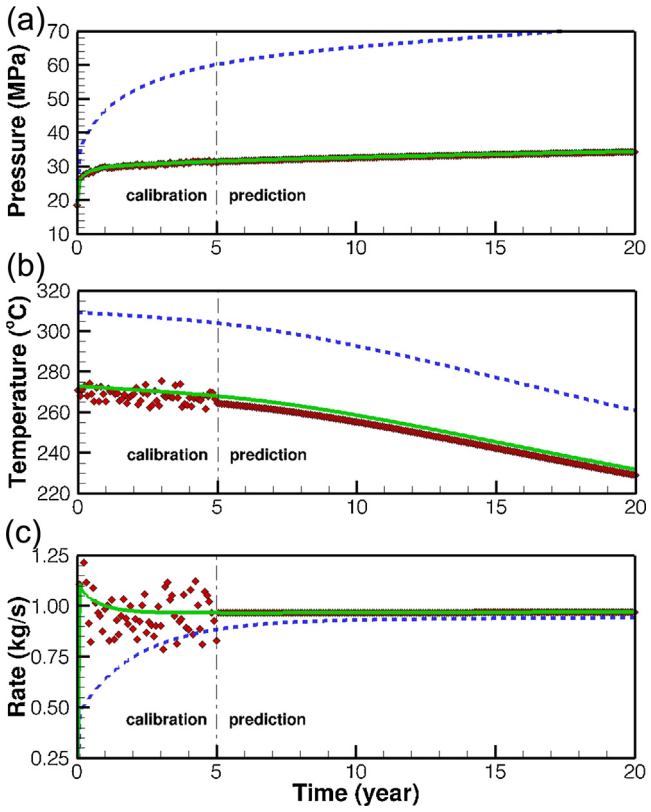

Fig. 12. (a) Injection pressure, (b) production temperature, and (c) production rates simulated with the uncalibrated model (dashed lines), and calibrated model (solid lines); the synthetic data used for model calibration during the first five years of production are shown as symbols.

Fig. 12 shows the true system behavior, the noisy synthetic observations used as calibration points during the first five years of production, the long-term system behavior, and the corresponding

Table 4
Results of sensitivity, residual, and data-worth analyses.

Observation	Injection pressure (bar)	Production rate (kg/s)	Production temperature (°C)
Composite sensitivity for inversion	1935.5	33.0	318.0
Mean residual	0.4	~0.0	−1.4
Standard deviation of residuals	1.8	0.1	3.1
Slope observed vs. calculated	1.0	0.9	0.7
Coefficient of determination	1.0	0.8	0.3
Contribution to objective function (%)	35.2	27.3	37.5
Data worth for inversion (%)	41.8	14.7	43.5
Data worth for prediction (%)	1.2	0.1	98.7

model predictions with the initial (i.e., uncalibrated) and calibrated models. It is obvious that even relatively minor errors in the two parameters examined here leads to grossly different predictions of reservoir behavior; a calibration step is thus essential. iTOUGH2 is capable of identifying the true parameter set within a few iterations, thus matching the calibration data and yielding a reasonable prediction of future reservoir behavior, specifically the considerable long-term temperature decline in the production well despite the near-by presence of a hot pluton.

This generic data inversion and associated analyses demonstrate that the newly developed equation-of-state module for sub- and supercritical water was successfully integrated into the iTOUGH2 simulation-inversion framework. It also indicates that simulating the deep heat source is essential, as it influences reservoir performance and the estimation of parameters that are correlated to the properties and conditions of, for example, an intrusion. Future analyses will take advantage of both the new simulation and related inversion and analysis capabilities to examine the behavior of high-temperature geothermal systems.

5. Conclusions

A new equation-of-state module, termed EOS1sc, was developed to extend the applicability of iTOUGH2 to temperatures and pressures above 800 °C and 100 MPa. Such extreme conditions are likely to occur in magmatic geothermal reservoirs where the heat sources can reach relatively shallow depths. EOS1sc has several advantages over other widely used geothermal simulators. These include a higher operational limit for temperature and pressure, faster computational speed, better accuracy, and/or inverse modeling capabilities.

Four versions of a five-spot geothermal problem were simulated, and results obtained by using the IAPWS-IF97 thermodynamic formulation were compared to those using the IAPWS-95 formulation. First, subcritical conditions and supercritical conditions close to the critical point were modeled and the results using IAPWS-IF97 and IAPWS-95 were identical. The former case was also compared to EOS1; both equation-of-state modules gave equal results. Then, supercritical problems were studied with high temperature and pressure conditions. The results demonstrated that the IAPWS-IF97 formulation with region 2 extrapolated deviates from the IAPWS-95 formulation, whereas the revised IAPWS-IF97 formulation with region 5 extrapolated gives equivalent results. Finally, a cooling pluton was modeled using IAPWS-IF97 in EOS1sc with region 5 extrapolated. The heat transfer in the reservoir was investigated as the pluton cools down until the reservoir reached steady-state. Results were compared to HYDROTHERM which gave equal results. In addition, an inverse analysis was performed to estimate the initial temperature of the pluton and the permeability of the geothermal reservoir.

Future work will further increase the applicability of EOS1sc to model the deep roots of geothermal systems by adding possibilities of temperature-dependent rock properties. That way, the brittle-ductile transition can be approximated by increasing the permeability of the intrusion as it cools down and becomes brittle. The temperature dependence of the rock thermal conductivity could also be modeled. In addition, the pluton's latent heat of crystallization can be approximated by increasing the heat capacity at high temperatures. Other future work includes adding IAPWS-IF97 to other equation-of-state modules in iTOUGH2, specifically those capable of modeling brine. Then, comprehensive magmatic geothermal reservoirs can be modeled and inverse modeling can be used to estimate some of the unknown parameters, answering questions relevant to field management of these supercritical systems.

Acknowledgments

Gratitude goes to the Geothermal Research Group (GEORG) for funding this study. The second author was supported, in part, by the U.S. Dept. of Energy under Contract No. DE-AC02-05CH11231.

References

Bouhifd, M.A., Besson, P., Courtial, P., Gérardin, C., Navrotsky, A., Richtet, P., 2007. Thermochemistry and melting properties of basalt. Contrib. Mineral. Petrol. 153, 689–698, http://dx.doi.org/10.1007/s00410-006-0170-8

Brikowski, T.H., 2001. Modeling supercritical systems with TOUGH2: preliminary results using the EOS1SC equation of state module. In: Proceedings, 26th Workshop on Geothermal Reservoir Engineering, Stanford University, Stanford, CA.

Clauser C., Huenges E., 1995. Thermal conductivity of rocks and minerals. In: Ahrens, T.J. (Ed.), Rock Physics and Phase Relations – a Handbook of Physical Constants, AGU Reference Shelf, vol. 3. American Geophysical Union, Washington, pp. 105–126.

Croucher, A.E., O'Sullivan, M.J., 2008. Application of the computer code TOUGH2 to the simulation of supercritical conditions in geothermal systems. Geothermics 37, 622–634, http://dx.doi.org/10.1016/j.geothermics.2008.03.005

Dausman, A.M., Doherty, J., Langevin, D.C., Sukop, M.C., 2010. Quantifying data worth toward reducing predictive uncertainty. Ground Water 48 (5), 729–740.

Elders, A., Fridleifsson, G., Albersson, A., 2014. Drilling into magma and the implications of the iceland deep drilling project (IDDP) for high-temperature geothermal systems worldwide. Geothermics 49, 111–118, http://dx.doi.org/10.1016/j.geothermics.2013.05.001

Finsterle, S., Kowalsky, M.B., 2008. Joint hydrological–geophysical inversion for soil structure identification. Vadose Zone J. 7, 287–293, http://dx.doi.org/10.2136/vzj2006.0078

Finsterle, S., Zhang, Y., 2011a. Solving iTOUGH2 simulation and optimization problems using the PEST protocol. Environ. Model. Softw. 26, 959–968, http://dx.doi.org/10.1016/j.envsoft.2011.02.008

Finsterle, S., Zhang, Y., 2011b. Error handling strategies in multiphase inverse modeling. Comput. Geosci. 37, 724–730, http://dx.doi.org/10.1016/j.cageo.2010.11.009

Finsterle, S., Zhang, Y., Pan, L., Dobson, P., Oglesby, K., 2013. Microhole arrays for improved heat mining from enhanced geothermal systems. Geothermics 47, 104–115, http://dx.doi.org/10.1016/j.geothermics.2013.03.001

Fridleifsson, G., Elders, A., 2005. The iceland deep drilling project: a search for deep unconventional geothermal resources. Geothermics 34, 269–285, http://dx.doi.org/10.1016/j.geothermics.2008.03.005

Fridleifsson, G., Palsson, B., Stefansson, B., Albertsson, A., Gunnlaugsson, E., Ketilsson, J., Lamarche, R., Andersen, P.E., 2010. Iceland Deep Drilling Project. The first IDDP drill hole drilled and completed in 2009. In: Proceedings, World Geothermal Congress, Bali, Indonesia.

Haar, L., Gallagher, J.S., Kell, G.S., 1984. NBS/NRC Steam Tables: Thermodynamic and Transport Properties and Computer Programs for Vapor and Liquid States of Water in SI units. Hemisphere Publishing Corp., New York, pp. 320.

Hayba, D.O., Ingebritsen, S.E., 1997. Multiphase groundwater flow near cooling plutons. J. Geophys. Res. 102, http://dx.doi.org/10.1029/97JB00552, 12,235–12,252.

Hayba, D.O., Ingebritsen, S.E., 1994. The Computer Model HYDROTHERM, a Three-Dimensional Finite-Difference Model to Simulate Ground-Water Flow and Heat Transport in the Temperature Range of 0–1200 °C, U.S. Geological Survey Water Resources Investigation 94-4045, Reston, VA.

Ingebritsen, S., Geiger, S., Hurwitz, S., Driesner, T., 2010. Numerical simulation of magmatic hydrothermal systems. Rev. Geophys. 48, RG1003, http://dx.doi.org/10.1029/2009RG000287

International Association for the Properties of Water and Steam: Revised Release on the IAPWS Industrial Formulation 1997 for the Thermodynamic Properties of Water and Steam. IAPWS Release, Switzerland, 2007.

International Association for the Properties of Water and Steam: Revised Release on the IAPWS Formulation 1995 for the Thermodynamic Properties of Ordinary Water Substance for General and Scientific Use. IAPWS Release, The Netherlands, 2009.

International Formulation Committee of the 6th International Conference on the Properties of Steam: The 1967 IFC Formulation for Industrial Use. Verein Deutscher Ingenieure, Düsseldorf, 1967.

Kissling, W.M., (PhD thesis) 2004. Deep Hydrology of the Geothermal Systems in the Taupo Volcanic Zone, New Zealand. University of Auckland, NZ.

Magnusdottir, L., Finsterle, S., 2015. Extending the applicability of the iTOUGH2 simulator to supercritical conditions. In: Proceedings, World Geothermal Congress, Melbourne, Australia.

Pritchett, J.W., 1995. STAR: a geothermal reservoir simulation system. In: Proceedings, World Geothermal Congress, Florence, Italy.

Pruess, K., Oldenburg, C.M., Moridis, G.J., 1999. TOUGH2 User's Guide Version 2. Lawrence Berkeley National Laboratory.

Pruess, K., 1991. TOUGH2 – A General Purpose Numerical Simulator for Multiphase Fluid and Heat Flow, Lawrence Berkeley Laboratory, Report LBL-29400, Berkeley, CA.

Wagner, W., Cooper, J.R., Dittman, A., Kijima, J., Kretzschmar, H.-J., Kruse, A., Mares, R., Oguchi, K., Sato, H., Stöcker, I., Sifner, O., Takaishi, Y., Tanishita, I., Trübenbach, J., Willkommen, Th., 2000. The IAPWS industrial formulation 1997 for the

thermodynamic properties of water and steam. J. Eng. Gas Turbines Power 122, 150–182, http://dx.doi.org/10.1115/1.483186
Wagner, W., Pruss, A., 2002. The IAPWS Formulation 1995 for the Thermodynamic Properties of Ordinary Water Substance for General and Scientific Use.
Wainwright, H.M., Finsterle, S., 2015. Global Sensitivity and Data-Worth Analyses in iTOUGH2, User's Guide, Report LBNL-TBD. Lawrence Berkeley National Laboratory, Berkeley, CA.
Weis, P., Driesner, T., Coumou, D., Geiger, S., 2014. Hydrothermal, multi-phase convection of H_2O-NaCl fluids from ambient to magmatic temperatures: a new numerical scheme and benchmarks for code comparison. Geofluids, http://dx.doi.org/10.1111/gfl.12080
Yamazaki, M., Muto, T., 2004. Extrapolation of IAPWS industrial formulation IAPWS-IF97 to high temperature above 800 °C. In: 14th International Conference on the Properties of Water and Steam in Kyoto.